



## VERIFICATION

I, Motoo AKAGI, a national of Japan, Nitto IPO Ltd.,  
No.17 Arai Bldg., 3-3, Shinkawa 1-chome, Chuo-ku, Tokyo 104-0033,  
Japan, verify that to the best of my knowledge and belief the  
following is a true translation made by me of the annexed document  
which is Japanese Patent Application, No. 2001-271770 filed on  
September 7, 2001.

Dated 28th day of June, 2004

Motoo Akagi

Motoo AKAGI, Translator

[Document Name]                    Application for Patent

[Reference No.]                    NT01P0429

[Application Date]                September 7, 2001

[Destination]                    Commissioner, Patent Office

[International Patent Classification]    G11B 5/66

[Inventor]

    [Address]    2880 Kozu, Odawara-shi, Kanagawa-ken,  
                  256-8510 Japan  
                  Hitachi, Ltd.,  
                  Data Storage Systems Division

    [Name]        Tetsuya KANBE

[Inventor]

    [Address]    2880 Kozu, Odawara-shi, Kanagawa-ken,  
                  256-8510 Japan  
                  Hitachi, Ltd.,  
                  Data Storage Systems Division

    [Name]        Hiroyuki SUZUKI

[Inventor]

    [Address]    2880 Kozu, Odawara-shi, Kanagawa-ken,  
                  256-8510 Japan  
                  Hitachi, Ltd.,  
                  Data Storage Systems Division

    [Name]        Yotsuo YAHISA

[Inventor]

    [Address]    280, 1-chome, Higashi-koigakubo,  
                  Kokubunji-shi, Tokyo  
                  Hitachi, Ltd.,  
                  Central Research Laboratory

    [Name]        Yoshiyuki HIRAYAMA

[Inventor]

[Address] 2880 Kozu, Odawara-shi, Kanagawa-ken,  
256-8510 Japan  
Hitachi, Ltd.,  
Data Storage Systems Division  
[Name] Hidekazu KASHIWASE

[Applicant for Patent]

[Identification No.] 000005108  
[Name] Hitachi, Ltd.

[Agent]

[Identification No.] 100068504  
[Patent Attorney] Katsuo OGAWA  
[Telephone No.] 03-3661-0071

[Agent]

[Identification No.] 100086656  
[Patent Attorney] Kyouusuke TANAKA  
[Telephone No.] 03-3661-0071

[Agent]

[Identification No.] 100094352  
[Patent Attorney] Ko SASAKI  
[Telephone No.] 03-3661-0071

[Designation of Charge]

[Ledger No. for Prepayment] 081423  
[Amount of Payment] 21000

[List of Document Submitted]

|               |               |    |
|---------------|---------------|----|
| [Object Name] | Specification | 01 |
| [Object Name] | Drawings      | 01 |
| [Object Name] | Abstract      | 01 |

[Proof] Required



[Type of the Document] Specification

[Title of the Invention]

MAGNETIC RECORDING MEDIUM AND MAGNETIC RECORDING  
APPARATUS

5 [What is claimed is]

[Claim 1]

A longitudinal magnetic recording medium  
characterized in that a magnetic layer is formed on a  
non-magnetic substrate via a plurality of underlayers,  
10 the magnetic layer comprises a lower magnetic layer  
containing at least one of Ru or Re in an amount of not  
less than 3 at% to not more than 30 at%, and Cr in an  
amount of not less than 0 at% to not more than 18 at%,  
and further containing at least one of B or C in an  
15 amount of not less than 0 at% to not more than 20 at%,  
and the balance being made up of Co, and an upper  
magnetic layer containing Co as a main component, anti-  
ferromagnetically coupled with the lower magnetic layer  
via a non-magnetic intermediate layer.

20 [Claim 2]

The longitudinal magnetic recording medium  
according to claim 1 characterized in that the  
plurality of the underlayers comprise a non-magnetic  
and amorphous structured first underlayer containing Co  
25 or Ni as a main component, and a body-centered cubic  
structured second underlayer containing Cr.

[Claim 3]

The longitudinal magnetic recording medium

according to claim 1 characterized in that the plurality of the underlayers comprise a first underlayer having a B2 structure, and a body-centered cubic structured second underlayer containing Cr.

5 [Claim 4]

The longitudinal magnetic recording medium according to claim 1 characterized in that at least one layer of the plurality of the underlayers is made of a non-magnetic and hexagonal close-packed structured alloy material containing Co.

10

[Claim 5]

The longitudinal magnetic recording medium according to claim 4 characterized in that the underlayer made of the non-magnetic and hexagonal close-packed structured alloy material containing Co is formed between the lower magnetic layer and the second underlayer.

15

[Claim 6]

The longitudinal magnetic recording medium according to claim 4 or claim 5 characterized in that the underlayer made of the non-magnetic and hexagonal close-packed structured alloy material containing Co is made of a Co-Ru alloy containing Ru in an amount of not less than 35 at% to not more than 60 at%.

20

[Claim 7]

The longitudinal magnetic recording medium according to any one of claims 1 to 6 characterized in that at least one layer of the plurality of the

25

underlayers is made of a body-centered cubic structured alloy material containing Cr, and the Cr alloy contains B in an amount of not less than 2 at% to not more than 15 at%.

5 [Claim 8]

A magnetic storage apparatus, comprising: a magnetic recording medium; a driver for driving it in the recording direction; a composite head having an inductive magnetic head for recording and a spin-valve  
10 type magnetic head for reading in combination; means for causing the head to perform relative movement with respect to the medium; and a read / write signal processing means with respect to the head, the magnetic recording medium being constituted by the longitudinal  
15 magnetic recording medium according to any one of claims 1 to 7.

[Detailed Description of the Invention]

[0001]

[Field of the Invention]

20 The present invention relates to a magnetic recording medium and a magnetic storage apparatus. More particularly, it relates to a technology of a longitudinal magnetic recording medium which has a low noise and a high coercivity, and is also sufficiently  
25 stable against thermal fluctuation. Further, it relates to a technology of a high reliability magnetic storage apparatus having an areal recording density of 50 megabits per square millimeter or more, which has

been implemented by combining the longitudinal magnetic recording medium technology with a technology of a high sensitivity magnetic head, and optimizing the read / write conditions.

5 [0002]

[Description of the Related Art]

In recent years, there is an increasingly growing demand for an improvement in areal recording density of a magnetic recording medium with an increase in capacity of a magnetic recording disk drive. A reduction in media noise is indispensable for improving the areal recording density. To that end, the grain size of a magnetic layer is required to be made fine for increasing the number of grains per bit. However, microfine magnetic crystal grains become more likely to undergo magnetization reversal due to the influence of thermal fluctuation. Accordingly, the decay of recorded magnetization, that is, the thermomagnetic relaxation phenomenon becomes noticeable. In order to suppress the thermomagnetic relaxation phenomenon, the thermal stability factor ( $K_u \cdot v / kT$ ) is required to be kept at generally 80 to 90 or more, wherein  $K_u$  is the crystal magnetic anisotropy constant,  $v$  is the volume of a magnetic crystal grain,  $k$  is the Boltzmann constant, and  $T$  is the absolute temperature. When the magnetic crystal grain has been made fine, the grain volume  $v$  is reduced. Accordingly,  $K_u$  is required to be raised for keeping  $K_u \cdot v / kT$  at not less than the

aforesaid value. If  $K_u$  is improved, the anisotropy field ( $H_k$ ) is also increased. However, if the  $H_k$  exceeds the recording magnetic field from a magnetic head, the overwrite characteristic is largely  
5 deteriorated. For this reason, the  $H_k$  of the medium is required to be set so as not to exceed the recording magnetic field from the head. This requirement results in the upper limit on the  $K_u$  value.

[0003]

10 As a technology for ensuring compatibility between the suppression of thermomagnetic relaxation and a reduction in noise, an anti-ferromagnetically coupled medium has been proposed in recent years (Appl. Phys. Lett., vol. 77, pp. 2581-2583, October (2000),  
15 and Appl. Phys. Lett., vol. 77, pp. 3806-3808, December (2000)). This medium is so configured that a magnetic layer portion has a double-layered structure in which respective magnetic layers are anti-ferromagnetically coupled via a Ru intermediate layer therebetween. In  
20 the anti-ferromagnetically coupled medium, the magnetization of a magnetic layer (lower magnetic layer) on the substrate side and the magnetization of another magnetic layer (upper magnetic layer) on the protective layer side are oriented in antiparallel to  
25 each other in the residual magnetization state. For this reason, when the product ( $B_r \cdot t$ ) of the residual magnetic flux density ( $B_r$ ) and the magnetic layer thickness ( $t$ ) is made equal to that of the medium using



a magnetic layer of a single-layered structure, it is possible to increase the thickness of the upper magnetic layer which is a recording layer. Thus, it is possible to raise the thermal stability factor ( $Ku \cdot v/kT$ ) of the magnetic layer.

[0004]

However, the foregoing technology falls short of specifically providing a longitudinal magnetic recording medium which has a low noise and a high coercivity, and is also sufficiently stable against thermal fluctuation.

[0005]

[Problems to be Solved by the Invention]

It is an object of the present invention to provide a longitudinal magnetic recording medium which has a low noise and a high coercivity, and is also sufficiently stable against thermal fluctuation. In addition, it is another object to provide a high reliability magnetic storage apparatus having an areal recording density of 50 megabits per square millimeter or more by combining the longitudinal magnetic recording medium with a high sensitivity magnetic head, and optimizing the read / write conditions.

[0006]

[Means for Solving the Problems]

In order to achieve the foregoing objects, in accordance with the present invention, the longitudinal magnetic recording medium has been so configured that a

magnetic layer is formed on a non-magnetic substrate via a plurality of underlayers, wherein the magnetic layer is made up of a lower magnetic layer containing at least one of Ru or Re in an amount of not less than 3 at% to not more than 30 at%, and Cr in an amount of not less than 0 at% to not more than 18 at%, and further containing at least one of B or C in an amount of not less than 0 at% to not more than 20 at%, and the balance being made up of Co, and an upper magnetic layer containing Co as a main component disposed thereon via a non-magnetic intermediate layer.

[0007]

Further, the plurality of the underlayers has been so configured as to include a non-magnetic and amorphous structured first underlayer containing Co or Ni as a main component, and a body-centered cubic structured second underlayer containing Cr.

[0008]

Further, a B2 structured alloy material may also be used for the first underlayer.

[0009]

Still further, at least one layer of the plurality of the underlayers has been so configured as to be made of a non-magnetic and hexagonal close-packed structured alloy material containing Co.

[0010]

Furthermore, it is also possible that the Co-containing alloy underlayer is formed as a third

underlayer between the lower magnetic layer and the second underlayer.

[0011]

5 Further, the underlayer made of a non-magnetic and hexagonal close-packed structured alloy material containing Co has been so configured as to be made of a Co-Ru alloy containing Ru in an amount of not less than 35 at% to not more than 60 at%.

[0012]

10 Still further, at least one layer of the plurality of the underlayers has been so configured as to be made of a Cr-containing body-centered cubic structured alloy material, wherein the Cr alloy contains B in an amount of not less than 2 at% to not  
15 more than 15 at%.

[0013]

Furthermore, in a magnetic storage apparatus having: a magnetic recording medium; a driver for driving it in the recording direction; a composite head  
20 having an inductive magnetic head for recording and a spin-valve type magnetic head for reading in combination; means for causing the head to perform relative movement with respect to the medium; and a read / write signal processing means with respect to  
25 the head, the magnetic recording medium has been allowed to be configured with the longitudinal magnetic recording medium.

[0014]

[Preferred Embodiments of the Invention]

First, a brief description will be given to the embodiments of the present invention.

In an anti-ferromagnetically coupled medium which  
5 is an example of a magnetic recording medium of the present invention, the product ( $Br \cdot t$ ) of the residual magnetic flux density ( $Br$ ) and the magnetic layer thickness ( $t$ ) is generally the difference between the  $Br \cdot t$  of an upper magnetic layer and the  $Br \cdot t$  of a lower  
10 magnetic layer. For this reason, when the  $Br \cdot t$  of the anti-ferromagnetically coupled medium is equally matched with the  $Br \cdot t$  of a single magnetic layer medium using the same magnetic alloy as that of the upper magnetic layer, the  $Br \cdot t$  of the upper magnetic layer  
15 may be set larger by the  $Br \cdot t$  of the lower magnetic layer. The  $Br \cdot t$  of the upper magnetic layer can be increased by mainly increasing the saturation magnetic flux density ( $B_s$ ) or the thickness of the magnetic layer. In the former case, it is possible to increase  
20 the crystal magnetic anisotropy constant ( $K_u$ ) if the anisotropy field ( $H_k$ ) is not reduced. In the latter case, it is possible to increase the volume of the crystal grain ( $v$ ). In consequence, it becomes possible to increase the thermal stability factor ( $K_u \cdot v / kT$ ) ( $k$ :  
25 Boltzmann constant, and  $T$ : the absolute temperature) of the upper magnetic layer. In the anti-ferromagnetically coupled medium, the upper magnetic layer serves as a recording layer. Therefore, by

improving the thermal stability of the magnetic layer,  
it is possible to suppress the thermomagnetic  
relaxation phenomenon.

[0015]

5           Accordingly, by setting the  $Br \cdot t$  of the lower  
magnetic layer at a large value, it is also possible to  
set the  $Br \cdot t$  of the upper magnetic layer at a large  
value. As a result, it is possible to more improve the  
thermal stability. However, in the anti-  
10   ferromagnetically coupled medium, the magnetization of  
the lower magnetic layer must be oriented in  
antiparallel to the magnetization of the upper magnetic  
layer in the residual magnetization state. To that end,  
the coercivity ( $H_{c2}$ ) of the lower magnetic layer is  
15   required to be made smaller than the coupled magnetic  
field ( $H_{ex2}$ ) applied on the lower magnetic layer. The  
 $H_{ex2}$  can be generally described as  $J/(Br \cdot t_2)$  by using  
the exchange coupling constant ( $J$ ) between the upper  
magnetic layer and the lower magnetic layer, and the  
20    $Br \cdot t$  ( $Br \cdot t_2$ ) of the lower magnetic layer. For this  
reason, the  $Br \cdot t_2$  is required to be not more than the  
 $J/H_{c2}$  for satisfying the foregoing conditions.  
Therefore, in order to increase the  $Br \cdot t_2$  as large as  
possible, it suffices that the  $J$  is increased, or that  
25   the  $H_{c2}$  is decreased.

[0016]

In order to decrease the  $H_{c2}$ , it is effective to  
use a material having a small anisotropy field ( $H_k$ ) for

the lower magnetic layer. The general materials currently used for the magnetic layer are hcp structured alloys each containing Co as a main component, and Cr, Pt, or the like, such as Co-Cr-Pt-B and Co-Cr-Pt-Ta alloys. The Hk of each of these Co alloys mainly depends upon the Pt content, so that it is possible to reduce the Hk by reducing the Pt content. [0017]

However, the atomic radius of Pt is larger as compared with that of Co by about 11 %. Therefore, when the Pt content of the lower magnetic layer is reduced, the lattice constant of the magnetic layer is also largely reduced at the same time. Since the upper magnetic layer contains Pt in an amount of 10 to 18 at% as described later, an extreme reduction in the Pt content of the lower magnetic layer results in a significant increase in degree of the lattice misfit between both the magnetic layers. As a result, the epitaxial growth of the upper magnetic layer is inhibited, thereby entailing the problem that the in-plane magnetic anisotropy is largely reduced. In order to prevent this problem, the material having a low Hk, but having a lattice constant which has not been largely reduced as compared with that of the upper magnetic layer is preferably used for the lower magnetic layer. The present inventors have conducted a study on various materials for the lower magnetic layer. As a result, they have found that the alloy containing

Co as a main component, and containing Ru or Re in place of Pt is most desirable. Although the atomic radius of each of Ru and Re is smaller than that of Pt, it is 68 % larger relative to that of Co.

5 [0018]

Further, even if each of these elements is alloyed with Co, the Hk is not increased. Therefore, the Co-Ru alloy or the Co-Re alloy can ensure the compatibility between a high lattice constant and a low  
10 Hk. As a result of the study, it has been indicated that the lower magnetic layer may contain Ru or Re in an amount of generally 3 at% or more in order not to inhibit the good epitaxial growth of the upper magnetic layer. However, when each of these elements is added  
15 in a large amount, the amount of magnetization of the lower magnetic layer is remarkably reduced. Therefore, the content is desirably 30 at% or less.

[0019]

Further, Cr may also be added in an amount of  
20 18 % or less in order to adjust the amount of magnetization. Since Cr has almost the same atomic radius as that of Co, it is capable of adjusting only the amount of magnetization without changing the lattice constant. However, if the amount of Cr added  
25 exceeds 18 %, the amount of magnetization is remarkably reduced. In consequence, the effect of canceling the Br·t of the upper magnetic layer is undesirably reduced.

[0020]

Further, since the grain size of the upper magnetic layer highly depends upon the grain size of the lower magnetic layer, it is possible to make fine the grain size of the upper magnetic layer by making fine the grain size of the lower magnetic layer. This case is preferable because the media noise can be reduced. In order to make fine the grain size of the lower magnetic layer, the magnetic layer desirably contains B or C in an amount of not less than 0 at% to not more than 20 at%. If the addition amount exceeds 20 at%, the crystalline structure of the lower magnetic layer undesirably undergoes remarkable deterioration. The thickness of the lower magnetic layer is desirably set at 1 nm or more. If it is less than 1 nm, the Br<sub>t</sub> of the lower magnetic layer is too small. Accordingly, the Br<sub>t</sub> of the upper magnetic layer cannot be set large enough for withstanding the thermal fluctuation. [0021]

Whereas, in general, when the lower magnetic layer is increased in thickness, the coercivity of the magnetic layer increases. For this reason, if the thickness exceeds a given value, the coercivity of the lower magnetic layer becomes larger than that of the coupled magnetic field applied on the magnetic layer. As a result, the magnetizations of the upper magnetic layer and the lower magnetic layer are not oriented in antiparallel to each other in the residual magnetization state. Consequently, the thickness at



this stage becomes the upper limit of the thickness of the lower magnetic layer. The lower magnetic layer of the present invention has an extremely low  $H_k$ , and hence it also has a low coercivity. Accordingly, even  
5 if it is increased in thickness to about 12 nm, it is possible to cause the magnetizations of the upper magnetic layer and the lower magnetic layer to be oriented in antiparallel to each other in the residual magnetization state. The correlation between the  
10 thickness of the lower magnetic layer and the electromagnetic transfer characteristic varies according to the material of the upper magnetic layer and the underlayer configuration. Therefore, it is desirable that the thickness of the lower magnetic  
15 layer is optimized within a range of 1 nm to 12 nm according to the media configuration.

[0022]

For the upper magnetic layer, it is desirable to use a hcp structured alloy containing Co as a main  
20 component, and containing Cr, Pt, B, or the like, such as CoCrPtB, CoCrPtTa, CoCrPtBCu, or CoCrPtBTa alloy. In order to sufficiently reduce the exchange interaction between magnetic grains, the Cr concentration of the upper magnetic layer is desirably  
25 14 at% or more. However, if the Cr concentration is increased, the crystal magnetic anisotropy constant ( $K_u$ ) is reduced, resulting in a decrease in thermal stability factor ( $K_u \cdot v/kT$ ). Therefore, the Cr content

is desirably 22 at% or less.

[0023]

Further, in order to ensure the compatibility between a high coercivity and a good overwrite characteristic, Pt is desirably contained therein in an amount of not less than 10 at% to not more than 18 at%. Still further, if B is added in an amount of 3 at% or more, the magnetic crystal grains are made fine, and at the same time, the grain boundary segregation of the Cr atoms is promoted. Accordingly, it is possible to largely reduce the media noise. However, since the addition of a large amount of B deteriorates the crystalline structure of the magnetic layer, the addition amount is desirably 18 at% or less. The media noise can also be reduced by adding Ta, Cu, Mo, Zr, W, Ti, SiO<sub>2</sub>, TiO<sub>2</sub>, ZrO<sub>2</sub>, Al<sub>2</sub>O<sub>3</sub>, or the like to the upper magnetic layer. The addition of each of the aforesaid elements or compounds disturbs the hcp structure of the magnetic layer. Therefore, the addition amount is preferably set at 10 at% or less, or 6 mol% or less.

[0024]

As the intermediate layer formed between the lower magnetic layer and the upper magnetic layer, a 0.2 nm - 0.8 nm-thick Ru layer is desirably used. If the Ru layer thickness departs from the aforesaid range, the anti-ferromagnetic coupling between the lower magnetic layer and the upper magnetic layer undesirably decays. As the materials for the intermediate layer,

any materials other than Ru present no problem so long as they are capable of introducing the anti-ferromagnetic coupling between the lower magnetic layer and the upper magnetic layer.

5 [0025]

As the layer configuration of the underlayer, for example, there may be adopted the multi-layered configuration in which a bcc structured second underlayer containing Cr is stacked on a first underlayer made of a non-magnetic and amorphous alloy containing Co, Ni, or the like as a main component. For the first underlayer, for example, there may be desirably used a Co-Crx1-Zry1 (x1: 30 to 60 at%, and y1: 3 to 30 at%), Ni-Crx2-Zry2 (x2: 0 to 50 at%, and y2: 3 to 60 at%), or Ni-Tax3-Zry3 (x3: 3 to 60 at%, and y3: 3 to 60 at%), Ni-Tax4 (x4: 5 to 60 at%) alloy, or the like. In this case, the grain size of the second underlayer is made fine, and at the same time, it is possible to cause the underlayer to exhibit such an orientation that the (100) plane is generally parallel to the substrate surface (hereinafter, referred to as (100) orientation).

20 [0026]

Therefore, the lower magnetic layer formed on the second underlayer exhibits such an orientation that the (11.0) plane is generally parallel to the substrate surface (hereinafter, referred to as (11.0) orientation) by epitaxial growth. The upper magnetic

layer also exhibits the (11.0) orientation via the intermediate layer. Accordingly, the grain size of the upper magnetic layer is made fine down to 11 nm or less, suitable for noise reduction, and at the same time, the c-axis in-plane component is improved. In consequence, it is possible to obtain a medium having a low noise and a strong in-plane magnetic anisotropy. The first underlayer is desirably non-magnetic. However, even if it has a slight magnetization, there is no problem from the practical viewpoint so long as the saturation magnetic flux density is 0.15 T or less.

[0027]

Further, the first underlayer is not required to have an accurate amorphous structure so long as it does not exhibit a distinct diffraction peak other than a halo pattern in the X-ray diffraction spectrum, or the mean grain size obtained from the lattice image photographed by a high resolution electron microscope is 5 nm or less. Even the materials for the first underlayer other than those described above have no particular restriction so long as they are the materials capable of causing the second Cr alloy underlayer to exhibit the (100) orientation, such as MgO, NiP, or Ta. Whereas, when a NiP-plated Al-Mg alloy is used for a substrate, the Cr alloy layer directly formed on the substrate is (100) oriented, so that particularly, the first underlayer is not required to be formed.

[0028]

For the second underlayer, there may be used bcc structured Cr, Cr-Ti alloy, Cr-Mo alloy, Cr-V alloy, Cr-W alloy, Cr-Mn alloy or the like. The Cr alloy is preferred since the lattice matching with the magnetic layer is improved because of its larger lattice constant as compared with that of pure Cr. Further, B may also be added thereto in order to make finer the grain size of the second underlayer. In this case, the grain size of the magnetic layer is also made finer, so that it is possible to further reduce the media noise. However, the addition of B deteriorates the crystalline structure of the underlayer simultaneously with making finer the grain size of the underlayer. Therefore, B is desirably added in an amount of 15 at% or less. Especially when the amount of B added exceeds 5 at%, for example, the second underlayer may also be configured in double layered structure by forming a Cr layer not containing B, and then forming a CrTiB layer thereon, or the like. As a result, it is possible to implement the underlayer which has ensured the compatibility between the microfine grain size and the strong (100) orientation.

[0029]

The lower magnetic layer may be formed directly on the second underlayer. Alternatively, a Co-containing hcp structured non-magnetic alloy layer may also be provided between the underlayer and the

magnetic layer as a third underlayer. In this case, the lower magnetic layer is epitaxially grown on the underlayer having the same crystal structure (hcp structure). Therefore, it undergoes good crystal growth from the initial growth state. For this reason, the crystalline structure of the upper magnetic layer and the in-plane orientation of the c-axis are also improved, so that it is possible to obtain a medium having a high coercivity. The material for the third underlayer has no particular restriction so long as it is an alloy material having a hcp structure and a saturation magnetic flux density of 0.15 T or less, such as a Co-Cr alloy or a Co-Cr-Pt alloy. However, when a Co-Ru alloy containing Ru in an amount of not less than 35 at% to not more than 60 at% is used, particularly desirably, the lattice matching is improved, so that it is possible to reduce the media noise.

[0030]

The aforesaid underlayer configuration causes all the magnetic layers to have the (11.0) orientation. However, the orientation of the magnetic layer may be the (10.0) orientation with the c-axis of the magnetic alloy facing in the in-plane direction as with the (11.0) orientation. In order for the magnetic layer to have the (10.0) orientation, a B2 structured alloy such as a Ni-50at% Al alloy may be desirably used for the first underlayer. In this case, the second underlayer

mainly exhibits the (211) orientation, and hence the third underlayer and the magnetic layer have the (10.0) orientation due to epitaxial growth. Even in the case in which the magnetic layer is (10.0)-oriented, the same effect as that for the (11.0) orientation can be obtained by using an alloy material containing Co as a main component, and containing Ru, Cr, B, or C of the present invention for the lower magnetic layer.

[0031]

By forming a nitrogen-doped carbon layer with a thickness of 3 nm to 7 nm as a protective layer, and further providing a lubricant layer of adsorptive perfluoroalkyl-polyether, or the like with a thickness of 1 nm to 4 nm, it is possible to obtain a high reliability magnetic recording medium capable of performing high density recording. Further, if a hydrogen-doped carbon layer, or a layer made of a compound such as silicon carbide, tungsten carbide, (W-Mo)-C, or (Zr-Nb)-N, or a mixed layer of any of the compounds and carbon is used as the protective layer, preferably, the durability against sliding and the corrosion resistance can be improved.

[0032]

As the substrate, there may be used, other than chemically strengthened aluminosilicate, ceramics made of soda-lime glass, silicon, borosilicate glass, or the like, glass-glazed ceramics, Ni-P non-electrolysis plated Al-Mg alloy substrate, or Ni-P sputtered glass

substrate, or rigid substrate made of Ni-P non-electrolysis plated glass, etc., or the like.

[0033]

As for the magnetic characteristics of the anti-ferromagnetically coupled medium of the present invention, it is desirable that the coercivity is not less than 240 kA/m (3,024 Oe) to not more than 400 kA/m (5,040 Oe), and that the residual magnetization ( $Br_t$ ) is not less than 2.0 Tnm (20G $\cdot\mu$ m) to not more than 6.0 Tnm (60G $\cdot\mu$ m). Herein, the residual magnetization is generally the value obtained by subtracting the  $Br_t$  of the lower magnetic layer from the  $Br_t$  of the upper magnetic layer, and it is the value corresponding to O $\cdot$ Q of FIG. 1. If the coercivity is less than 240 kA/m, the recording resolution is reduced. Whereas, if it exceeds 400 kA/m, the overwrite characteristic is deteriorated. Thus, both the cases are undesirable.

[0034]

Further, if the residual magnetization is less than 2.0 Tnm, the read output is reduced. Whereas, if it exceeds 6.0 Tnm, high resolution cannot be obtained. Thus, both the cases are undesirable.

[0035]

The graph of FIG. 1 shows one example of the hysteresis loop of the anti-ferromagnetically coupled medium of the present invention. The magnetization of the lower magnetic layer is required to be oriented in antiparallel to the magnetization of the upper magnetic



layer in the residual magnetization state. For this reason, the magnetic field at which the magnetization reversal of the lower magnetic layer is completed (point P in the figure) must be a positive value.

5 Further, in order to sufficiently suppress the thermomagnetic relaxation phenomenon, the thermal stability factor ( $K_u \cdot v / kT$ ) is desirably 80 to not less than 90. The thermal stability factor can be determined by fitting the time dependence of the  
10 remanence coercivity in the Sharrock's equation as described in, J. Magn. Magn. Mater. 127, p. 233 (1993), for example. From the study by the present inventors, it has been concluded as follows: if the  $K_u \cdot v / kT$  at room temperature determined in this manner is 80 to not  
15 less than 90, the decay in read output at 5 years later is estimated to be 10 % or less, thus presenting no problem in terms of reliability.

[0036]

Further, in a magnetic storage apparatus having a  
20 magnetic recording medium, a driver for driving it in the recording direction, a magnetic head made up of a write element and a read element, means for causing the magnetic head to perform relative movement with respect to the magnetic recording medium, and a read / write  
25 signal processing means for performing the signal input to the magnetic head and the output signal read-back from the magnetic head, by using any of the aforesaid media for the magnetic recording medium, it is possible

to provide a high reliability magnetic storage apparatus having an areal recording density of 50 Mbit/mm<sup>2</sup> or more.

[0037]

5           Namely, the read element of the magnetic head is configured with a spin-valve type sensor including a plurality of conductive magnetic layers of which mutual magnetization directions are relatively changed by the external magnetic field to generate a large resistance  
10 change, and conductive non-magnetic layers disposed each between the conductive magnetic layers. The sensor element is desirably formed between the two shield layers made of a soft magnetic material separated by a distance of 0.10  $\mu\text{m}$  or less from one  
15 another. This is attributable to the following fact. Namely, if the distance between shields is 0.10  $\mu\text{m}$  or more, the resolution is reduced, so that the phase jitter of a signal increases. By implementing the aforesaid configuration of the storage apparatus, it is  
20 possible to further raise the signal intensity. As a result, it becomes possible to implement a high reliability magnetic storage apparatus having a recording density of 50 Mbit/mm<sup>2</sup> or more.

[0038]

25           Below, the detailed examples of the present invention will be further described in details by reference to drawings.

<Example 1>

FIG. 2 is a cross sectional view of the configuration of one embodiment of a magnetic recording medium of the present invention. As a substrate 11, a 0.635 mm-thick and 2.5-dia type aluminosilicate glass substrate of which surface had been chemically strengthened was used. This substrate was subjected to alkali cleaning. Subsequently, the following multi-layered film was formed with a tact of 9 sec by means of a sheet-fed type sputtering apparatus (NDP250B) manufactured by Intervac Co. The chamber configuration or the station configuration of this sputtering apparatus is shown in FIG. 3. First, in a charging chamber 20, the substrate 11 was kept under vacuum, and in a first underlayer forming chamber 21, first underlayers 12 each made of a 30 nm-thick Ni-37.5at% Ta alloy were formed on both the sides of the substrate 11. Thereafter, in a heating chamber 22, heating was conducted in a mixed gas atmosphere of an Ar gas and oxygen by a lamp heater so that the temperature of the substrate is about 240 °C. In a second underlayer forming chamber 23, second underlayers 13 each made of a 10 nm-thick Cr-20at% Ti alloy were formed respectively thereon.

[0039]

Further, subsequently, in a third underlayer forming chamber 24, third underlayers 14 each made of a 3 nm-thick Co-40at% Ru alloy were formed respectively thereon. Then, in a lower magnetic layer forming

chamber 25, lower magnetic layers 15 each made of a 2 to 10 nm-thick Co-24at% Ru-8at% B alloy were formed respectively thereon. In an intermediate layer forming chamber 26, 0.4 nm-thick Ru intermediate layers 16 were formed respectively thereon. Then, in an upper magnetic layer forming chamber 27, 18 nm to 21 nm-thick upper magnetic layers 17 each made of Co-18at% Cr-14at% Pt-8at% B alloy were formed respectively thereon. In two protective layer forming chambers 28 and 28', protective layers 18 each having a total thickness of 4 nm were formed respectively thereon. Table 1 shows the combinations of the thickness of the lower magnetic layer and the thickness of the upper magnetic layer. Subsequently, the substrate was taken out from the sputtering apparatus. Then, a lubricant containing perfluoroalkyl-polyether as a main component was applied on the protective layers to form 1.8 nm-thick lubricant layers 19.

[0040]

For forming the first underlayers 12, the second underlayers 13, the third underlayers 14, the lower magnetic layers 15, the intermediate layers 16, and the upper magnetic layers 17, Ar was used as a discharge gas in all the cases. The gas pressure was set at 5.3 Pa (40 mTorr) only for depositing the lower magnetic layers, and at 0.93 Pa (7 mTorr) for depositing other layers. Further, for forming the protective layers 18 made of carbon, Ar containing nitrogen was used as the

discharge gas, and the pressure thereof was set at 1.33 Pa (10 mTorr).

[0041]

The magnetic recording medium formed in this manner was cut, and the laminated thin film portion was reduced in thickness in a mortar form vertically along the direction perpendicular to the layer surface by an ion thinning method. Thus, the microfine structure of the first underlayer was observed by means of a transmission electron microscope with an acceleration voltage of 200 kV. As a result, the crystal grain size was found to be 5 nm or less. Further, upon photographing the selected-area electron diffraction image, a halo was observed. Accordingly, it has been confirmed that the structure is substantially an amorphous structure.

[0042]

The magnetic characteristics of the magnetic disk medium obtained were evaluated by a coercivity measuring apparatus utilizing the Kerr effect and a vibrating sample magnetometer (VSM). From the magnetic disk, 8 mm square samples were cut to be used as test samples for VSM. The measurement of the magnetic characteristics by VSM was carried out at room temperature by applying a magnetic field of up to 800 kA/m at maximum in the circumferential direction of the medium. Table 2 shows the magnetic characteristics corresponding to their respective sample Nos. shown in

Table 1. The coercivities  $H_c$  determined by using the Kerr effect were less than 300 kA/m for the sample Nos. 101, 102, and 106. For the samples having coercivities in excess of 300 kA/m, the magnetic characteristics were evaluated by VSM. The thermal stability factor ( $K_u \cdot v/kT$ ) was determined by approximating the time dependence of the remanence coercivity at 7.5 sec to 240 sec at room temperature to the Sharrock's equation. Incidentally, the measurements of the remanence coercivity were carried out for 6 points at 7.5, 15, 30, 60, 120, and 240 sec later.

[0043]

Table 1

| Sample No. | Lower magnetic layer    | Intermediate layer | Upper magnetic layer             |
|------------|-------------------------|--------------------|----------------------------------|
|            | Co-24at% Ru-8at% B (nm) | Ru (nm)            | Co-18at% Cr-14at% Pt-8at% B (nm) |
| 101        | 10.0                    | 0.4                | 18.0                             |
| 102        | 8.0                     | ↑                  | 18.0                             |
| 103        | 6.0                     | ↑                  | 18.0                             |
| 104        | 4.0                     | ↑                  | 18.0                             |
| 105        | 2.0                     | ↑                  | 18.0                             |
| 106        | 10.0                    | ↑                  | 19.5                             |
| 107        | 8.0                     | ↑                  | 19.5                             |
| 108        | 6.0                     | ↑                  | 19.5                             |
| 109        | 4.0                     | ↑                  | 19.5                             |
| 110        | 2.0                     | ↑                  | 19.5                             |
| 111        | 10.0                    | ↑                  | 21.0                             |
| 112        | 8.0                     | ↑                  | 21.0                             |
| 113        | 6.0                     | ↑                  | 21.0                             |
| 114        | 4.0                     | ↑                  | 21.0                             |
| 115        | 2.0                     | ↑                  | 21.0                             |

Table 2

| Sample No. | Kerr      | VSM       |      |             |         |
|------------|-----------|-----------|------|-------------|---------|
|            | Hc (kA/m) | Hc (kA/m) | S*   | Br·t (T·nm) | Ku·v/kT |
| 101        | 241       | -         | -    | -           | -       |
| 102        | 264       | -         | -    | -           | -       |
| 103        | 328       | 249       | 0.83 | 2.7         | 79      |
| 104        | 328       | 276       | 0.70 | 3.9         | 84      |
| 105        | 334       | 295       | 0.71 | 4.8         | 83      |
| 106        | 260       | -         | -    | -           | -       |
| 107        | 320       | 237       | 0.68 | 2.1         | 81      |
| 108        | 331       | 249       | 0.59 | 3.2         | 84      |
| 109        | 333       | 289       | 0.73 | 4.3         | 87      |
| 110        | 339       | 306       | 0.74 | 5.5         | 90      |
| 111        | 319       | 187       | 0.50 | 1.9         | 78      |
| 112        | 333       | 240       | 0.72 | 2.4         | 84      |
| 113        | 334       | 270       | 0.72 | 3.5         | 85      |
| 114        | 334       | 290       | 0.70 | 5.2         | 93      |
| 115        | 339       | 304       | 0.72 | 5.9         | 93      |

Not depending upon the thickness of the upper magnetic layer, if the thickness of the lower magnetic layer was increased, the coercivity, the product (Br·t) of the residual magnetic flux density Br and the thickness t of the magnetic layer, the thermal stability factor (Ku·v/kT), and the like were reduced. For example, in the medium in which the thickness of the upper magnetic layer had been set at 21 nm, when the thickness of the lower magnetic layer was increased up to 2 nm to 10 nm, the coercivity decreased to 304 kA/m to 187 kA/m, the Br·t decreased to 5.9 Tnm to 1.9 Tnm, and the Ku·v/kT decreased to 93 to 78, respectively. FIG. 4 shows the enlarged view of a portion at a magnetic field of around zero of each

hysteresis loop of the sample Nos. 111 to 114. For any of the media, steps are observed in the hysteresis loop in the area in which the magnetic field is positive (upper right quadrant region).

5 [0044]

This indicates as follows. When the magnetic field has been set at zero, the magnetization reversal of the lower magnetic layer is completed. Thus, in the residual magnetization state, the magnetization of the lower magnetic layer is oriented in antiparallel to the magnetization of the upper magnetic layer. In consequence, it has been shown that, in each of the media of this example, even if the thickness of the lower magnetic layer is increased to 10 nm, the magnetizations of the upper magnetic layer and the lower magnetic layer are oriented in antiparallel to each other in the residual magnetization state.

15 [0045]

The evaluation of the electromagnetic transfer characteristics was carried out by using a composite head made up of a GMR head having a shield gap length of 0.10  $\mu\text{m}$  and a track width for read (Twr) of 0.33  $\mu\text{m}$ , and a writing head having a gap length of 0.14  $\mu\text{m}$ . The linear recording density which was 1/6 the maximum linear recording density (HF) was set for 1F of the overwrite characteristic, wherein the maximum linear recording density (HF) was 24.8 kFC/mm (630 kFCI). The electromagnetic transfer characteristics corresponding



to the sample Nos. shown in Table 1 are shown in Table 3. If the lower magnetic layer is increased in thickness not depending upon the thickness of the upper magnetic layer, the output half-width (PW50) of the solitary reproduction wave decreased, and the output resolution (ReMF) at the linear recording density (MF) which was half the maximum linear recording density was improved. Further, at this step, the overwrite characteristic (OW) was also improved.

[0046]

Table 3

| Sample No. | So<br>( $\mu$ Vpp) | PW50<br>(nm) | OW<br>(dB) | ReMF<br>(%) | Nd/So<br>( $\mu$ Vrms/ $\mu$ Vpp) | Media<br>S/N (dB) |
|------------|--------------------|--------------|------------|-------------|-----------------------------------|-------------------|
| 103        | 954                | 116          | 42         | 53.3        | 0.0417                            | 22.1              |
| 104        | 1250               | 120          | 37         | 49.0        | 0.0384                            | 22.1              |
| 105        | 1486               | 123          | 36         | 48.8        | 0.0394                            | 21.9              |
| 108        | 1055               | 117          | 41         | 51.2        | 0.0391                            | 22.3              |
| 109        | 1375               | 123          | 36         | 47.6        | 0.0384                            | 21.9              |
| 110        | 1592               | 125          | 36         | 47.9        | 0.0391                            | 21.8              |
| 113        | 1163               | 118          | 40         | 50.9        | 0.0384                            | 22.4              |
| 114        | 1440               | 124          | 36         | 47.3        | 0.0398                            | 21.5              |
| 115        | 1640               | 127          | 35         | 47.9        | 0.0412                            | 21.3              |

On the other hand, the normalized media noise (Nd/So) obtained by normalizing the media noise (Nd) when recording was performed at HF with a solitary reproduction wave output (So) exhibited different lower magnetic layer thickness dependencies according to the thickness of the upper magnetic layer. In the case where the lower magnetic layer thickness was increased to 2 nm to 6 nm when the thickness of the upper magnetic layer was 18.0 nm, the Nd/So increased about

6 %. In contrast, it decreased about 7 % when the thickness of the upper magnetic layer was 21.0 nm. Further, the media S/N showed the highest value when the upper magnetic layer thickness was set at 21 nm, and the lower magnetic layer thickness was increased to 6 nm. Herein, the media S/N is the value defined as  $\text{media S/N} = 20 \log (\text{SMF}/\text{Nd})$  by using the read output at MF (SMF) and Nd.

[0047]

When a Co-32at% Cr-6at% Zr, Co-36at% Cr-8at% Ta, Co-40at% V-8at% B, or Co-50at% V-12at% Si alloy was used in place of the Ni-37.5at% Ta alloy for the first underlayer, in combination with the magnetic layer of the sample No. 113, a particularly low normalized noise was shown. Further, for the medium using a Ni-40at% Cr-8at% Zr, or Ni-55at% V-15at% Si alloy for the first underlayer, a particularly high coercivity of 360 kA/m or more was obtained.

[0048]

#### <Example 2>

Media each having the same layer configuration as that in Example 1, except that a Co-24at% Ru-10at% B alloy was used as the lower magnetic layer were formed through the same deposition process as that in Example 1. Table 4 shows the combinations of the thickness of the lower magnetic layer and the thickness of the upper magnetic layer, and Table 5 shows the magnetic characteristics thereof. From the comparison between

the magnetic characteristics shown in Tables 2 and 5,  
it has been shown that, when the same thickness is  
adopted for each upper magnetic layer, use of the Co-  
24at% Ru-10at% B alloy provides larger  $H_c$ ,  $Br_t$ , and  
5  $K_u \cdot V/kT$  than with the use of Co-24at% Ru-8at% B alloy  
for the lower magnetic layer.

[0049]

The electromagnetic transfer characteristics of  
disks having their respective magnetic characteristics  
10 of Table 5 were evaluated by using the magnetic head  
used for the disk evaluation in Example 1. As a result,  
as shown in Table 6, it has been shown as follows.  
Namely, when the Co-24at% Ru-10at% B has been used for  
the lower magnetic layer, if the thickness of the lower  
15 magnetic layer is increased to 2 nm to 6 nm, not  
depending upon the thickness of the upper magnetic  
layer, (1) PW50 shortens; (2) the overwrite  
characteristic and the media S/N are improved; and (3)  
the Nd/So decreases. Especially when the thickness of  
20 the upper magnetic layer has been set at 21 nm, the  
decrease in Nd/So is noticeable.

[0050]

Table 4

| Sample No. | Lower magnetic layer        | Intermediate layer | Upper magnetic layer                |
|------------|-----------------------------|--------------------|-------------------------------------|
|            | Co-24at% Ru-10at% B<br>(nm) | Ru<br>(nm)         | Co-18at% Cr-14at%<br>Pt-8at% B (nm) |
| 201        | 10.0                        | 0.4                | 18.0                                |
| 202        | 8.0                         | ↑                  | 18.0                                |
| 203        | 6.0                         | ↑                  | 18.0                                |
| 204        | 4.0                         | ↑                  | 18.0                                |
| 205        | 2.0                         | ↑                  | 18.0                                |
| 206        | 10.0                        | ↑                  | 19.5                                |
| 207        | 8.0                         | ↑                  | 19.5                                |
| 208        | 6.0                         | ↑                  | 19.5                                |
| 209        | 4.0                         | ↑                  | 19.5                                |
| 210        | 2.0                         | ↑                  | 19.5                                |
| 211        | 10.0                        | ↑                  | 21.0                                |
| 212        | 8.0                         | ↑                  | 21.0                                |
| 213        | 6.0                         | ↑                  | 21.0                                |
| 214        | 4.0                         | ↑                  | 21.0                                |
| 215        | 2.0                         | ↑                  | 21.0                                |

Table 5

| Sample No. | Kerr         | VSM          |      |                |         |
|------------|--------------|--------------|------|----------------|---------|
|            | Hc<br>(kA/m) | Hc<br>(kA/m) | S*   | Br·t<br>(T·nm) | Ku·v/kT |
| 201        | 227          | -            | -    | -              | -       |
| 202        | 260          | -            | -    | -              | -       |
| 203        | 318          | 252          | 0.77 | 3.2            | 81      |
| 204        | 324          | 268          | 0.77 | 4.3            | 84      |
| 205        | 336          | 308          | 0.75 | 5.2            | 90      |
| 206        | 311          | -            | -    | -              | -       |
| 207        | 316          | 237          | 0.69 | 2.8            | 81      |
| 208        | 321          | 253          | 0.75 | 3.8            | 84      |
| 209        | 329          | 283          | 0.73 | 5.0            | 89      |
| 210        | 341          | 309          | 0.74 | 6.1            | 93      |
| 211        | 313          | 206          | 0.54 | 2.3            | 82      |
| 212        | 321          | 254          | 0.70 | 3.4            | 86      |
| 213        | 324          | 277          | 0.73 | 4.4            | 93      |
| 214        | 328          | 287          | 0.73 | 5.7            | 94      |
| 215        | 342          | 319          | 0.73 | 6.8            | 99      |

Table 6

| Sample No. | So<br>( $\mu\text{Vpp}$ ) | PW50<br>(nm) | OW<br>(dB) | ReMF<br>(%) | Nd/So<br>( $\mu\text{Vrms}/\mu\text{Vpp}$ ) | Media<br>S/N (dB) |
|------------|---------------------------|--------------|------------|-------------|---|-------------------|
| 203        | 1072                      | 119          | 41         | 50.7        | 0.0369                                      | 22.8              |
| 204        | 1346                      | 123          | 37         | 47.8        | 0.0396                                      | 21.6              |
| 205        | 1559                      | 125          | 36         | 47.9        | 0.0393                                      | 21.7              |
| 208        | 1231                      | 120          | 39         | 48.7        | 0.0351                                      | 22.8              |
| 209        | 1507                      | 125          | 35         | 47.1        | 0.0390                                      | 21.6              |
| 210        | 1681                      | 126          | 36         | 47.6        | 0.0398                                      | 21.6              |
| 213        | 1370                      | 123          | 38         | 48.0        | 0.0347                                      | 22.8              |
| 214        | 1608                      | 128          | 35         | 46.4        | 0.0402                                      | 21.2              |
| 215        | 1781                      | 129          | 34         | 46.8        | 0.0413                                      | 21.1              |

## &lt;Example 3&gt;

Media each having the same layer configuration as that in Example 1 were formed, except for changing (1) the substrate temperature, (2) the thickness of the CrTi underlayer, and (3) the thickness of the Ru intermediate layer. The deposition process was the same as that in Example 1, except that the Ar gas pressure during deposition of the lower magnetic layer was set at 0.93 Pa. Tables 7 to 9 show the relationship between the layer configuration of each medium and the sample number, the magnetic characteristics, and the electromagnetic transfer characteristics. Incidentally, a head having a  $T_{wr} = 0.35 \mu\text{m}$  was used for the evaluation of the electromagnetic transfer characteristics. Any of the media showed a high coercivity of 260 kA/m or more, and a low normalized media noise of  $0.04 \mu\text{Vrms}/\mu\text{Vpp}$  or less.

[0051]

Table 7

| Sample No. | Substrate temperature (°C) | Second underlayer Cr-20at% Ti (nm) | Lower magnetic layer Co-24at% Ru-8at% B (nm) | Intermediate layer Ru (nm) | Upper magnetic layer Co-18at% Cr-14at% Pt-8at% B (nm) |
|------------|----------------------------|------------------------------------|--|----------------------------|---|
| 301        | 210                        | 10                                 | 2.0  | 0.4                        | 18.0  |
| 302        | 240                        | 10                                 | ↑  | ↑                          | ↑   |
| 303        | 270                        | 15                                 | ↑  | ↑                          | ↑   |
| 304        | ↑                          | 5                                  | ↑  | ↑                          | ↑   |
| 305        | ↑                          | 10                                 | ↑  | 0.8                        | ↑   |
| 306        | ↑                          | ↑                                  | ↑  | 0.6                        | ↑   |
| 307        | ↑                          | ↑                                  | ↑  | 0.4                        | ↑   |
| 308        | ↑                          | ↑                                  | ↑  | 0.2                        | ↑   |
| 309        | 300                        | ↑                                  | ↑  | ↑                          | ↑   |

Table 8

| Sample No. | Hc (kA/m) | S*   | Br·t (T·nm) | Ku·v/kT |
|------------|-----------|------|-------------|---------|
| 301        | 264       | 0.80 | 5.0         | 78      |
| 302        | 298       | 0.72 | 5.1         | 88      |
| 303        | 338       | 0.72 | 5.2         | 105     |
| 304        | 295       | 0.66 | 5.4         | 89      |
| 305        | 317       | 0.63 | 5.4         | 101     |
| 306        | 326       | 0.70 | 5.4         | 100     |
| 307        | 331       | 0.68 | 5.2         | 103     |
| 309        | 345       | 0.69 | 4.8         | 118     |

5

Table 9

| Sample No. | So (μVpp) | PW50 (nm) | OW (dB) | ReMF (%) | Nd/So (μVrms/μVpp) | Media S/N (dB) |
|------------|-----------|-----------|---------|----------|--------------------|----------------|
| 301        | 1107      | 125.7     | 37      | 48       | 0.0400             | 21.6           |
| 302        | 1132      | 125.2     | 36      | 48       | 0.0372             | 22.3           |
| 303        | 1097      | 125.2     | 36      | 49       | 0.0391             | 22.0           |
| 304        | 1153      | 126.6     | 36      | 48       | 0.0356             | 22.6           |
| 305        | 1154      | 128.1     | 35      | 48       | 0.0379             | 22.0           |
| 306        | 1116      | 126.8     | 35      | 48       | 0.0385             | 21.9           |
| 307        | 1127      | 125.4     | 35      | 48       | 0.0384             | 22.0           |
| 309        | 1059      | 125.3     | 35      | 49       | 0.0378             | 22.2           |

The Hc and the Ku·v/kT tended to increase with an

increase in substrate temperature, but that the media S/N became maximum when the substrate temperature was 240 °C. The Hc and the  $K_u \cdot V/kT$  increased also when the CrTi underlayer was increased in thickness. The  
5 Nd/So of the medium (sample No. 304) in which the thickness of the CrTi underlayer had been decreased to 5 nm was minimum, indicating that a decrease in thickness of the CrTi underlayer is effective for noise reduction. On the other hand, the change in  
10 electromagnetic transfer characteristics with the change in thickness of the Ru intermediate layer was small, and the characteristics were generally constant within a range of 0.2 to 0.8 nm. Whereas, for evaluating the magnetic characteristics of the Co-24at%  
15 Ru-8at% B alloy used for the lower magnetic layer, a medium in which the thickness of the magnetic layer had been set at 18 nm and the upper magnetic layer had not been formed was manufactured. The magnetization curve was measured by applying a magnetic field in the in-  
20 plane direction. As a result, the coercivity and the saturation magnetic flux density were 8.8 kA/m and 0.60 T, respectively.

[0052]

<Example 4>

25 Media each having the same layer configuration as that in Example 2 were formed, except for changing (1) the substrate temperature, (2) the thickness of the CrTi underlayer, and (3) the thickness of the Ru

intermediate layer. Tables 10 to 12 show the relationship between the layer configuration of each medium and the sample number, the magnetic characteristics, and the electromagnetic transfer characteristics evaluated by the head used in Example 3, respectively. Any of the media showed a high Hc of 250 kA/m or more, and a high media S/N of 21.5 dB or more. As with Example 3, both of the Hc and the Ku·v/kT increased with an increase in substrate temperature and an increase in thickness of the CrTi underlayer. However, both values of the Hc and the Ku·v/kT were slightly smaller as compared with those of the media of Example 3. Further, the medium (sample No. 404) in which the thickness of the CrTi underlayer had been decreased to 5 nm had the lowest noise, and had the maximum media S/N.

[0053]

Table 10

| Sample No. | Substrate temperature (°C) | Second underlayer Cr-20at% Ti (nm) | Lower magnetic layer Co-24at% Ru-10at% B (nm) | Intermediate layer Ru (nm) | Upper magnetic layer Co-18at% Cr-14at% Pt-8at% B (nm) |
|------------|----------------------------|------------------------------------|---|----------------------------|---|
| 401        | 210                        | 10                                 | 2.0   | 0.4                        | 18.0  |
| 402        | 240                        | 10                                 | ↑   | ↑                          | ↑   |
| 403        | 270                        | 15                                 | ↑   | ↑                          | ↑   |
| 404        | ↑                          | 5                                  | ↑   | ↑                          | ↑   |
| 405        | ↑                          | 10                                 | ↑   | 0.8                        | ↑   |
| 406        | ↑                          | ↑                                  | ↑   | 0.6                        | ↑   |
| 407        | ↑                          | ↑                                  | ↑   | 0.4                        | ↑   |
| 408        | ↑                          | ↑                                  | ↑   | 0.2                        | ↑   |
| 409        | 300                        | ↑                                  | ↑   | ↑                          | ↑   |



Table 11

| Sample No. | Hc<br>(kA/m) | S*   | Br·t<br>(T·nm) | Ku·v/kT |
|------------|--------------|------|----------------|---------|
| 401        | 254          | 0.80 | 5.5            | 71      |
| 402        | 286          | 0.68 | 5.4            | 84      |
| 403        | 322          | 0.71 | 5.3            | 103     |
| 404        | 281          | 0.69 | 5.3            | 85      |
| 405        | 318          | 0.69 | 5.4            | 100     |
| 406        | 312          | 0.64 | 5.4            | 99      |
| 407        | 314          | 0.60 | 5.6            | 99      |
| 409        | 336          | 0.68 | 5.5            | 115     |

Table 12

| Sample No. | So<br>( $\mu$ Vpp) | PW50<br>(nm) | OW<br>(dB) | ReMF<br>(%) | Nd/So<br>( $\mu$ Vrms/ $\mu$ Vpp) | Media<br>S/N (dB) |
|------------|--------------------|--------------|------------|-------------|-----------------------------------|-------------------|
| 401        | 1197               | 128          | 36         | 48          | 0.0399                            | 21.5              |
| 402        | 1179               | 128          | 35         | 48          | 0.0364                            | 22.3              |
| 403        | 1117               | 128          | 35         | 49          | 0.0387                            | 22.0              |
| 404        | 1181               | 127          | 36         | 47          | 0.0349                            | 22.5              |
| 405        | 1164               | 129          | 35         | 48          | 0.0372                            | 22.1              |
| 406        | 1130               | 128          | 35         | 48          | 0.0376                            | 22.2              |
| 407        | 1151               | 127          | 35         | 48          | 0.0371                            | 22.2              |
| 409        | 1122               | 128          | 35         | 48          | 0.0379                            | 22.0              |

As for the media of this example, there were not  
5 observed large differences in electromagnetic transfer  
characteristics as compared with those of the media of  
Example 3. The coercivity and the saturation magnetic  
flux density of the Co-24at% Ru-10at% B alloy used for  
the lower magnetic layer were determined in the same  
10 manner as in Example 3, and found to be 7.6 kA/m and  
0.56 T, respectively.

[0054]

#### <Example 5>

The media in each of which a 25 nm-thick Co-30at%  
15 Cr-10at% Zr alloy layer was used as the first

underlayer, and a Co-20at% Cr-14at% Pt-6at% B alloy layer was used as the upper magnetic layer were manufactured. The layer configuration and the deposition process are the same as in Example 1. Table 13 shows the set values of (1) the substrate temperature, (2) the thickness of the second underlayer, (3) the thickness of the lower magnetic layer, (4) the thickness of the Ru intermediate layer, and (5) the thickness of the upper magnetic layer. Table 14 shows the respective magnetic characteristics corresponding to the media. The  $K_u \cdot v / kT$  increases up to 330 °C with an increase in substrate temperature, but the coercivity tends to be saturated at 300 °C or more. Further, the coercivity squareness  $S^*$  of each medium of this example was smaller as compared with the  $S^*$  of each medium of examples shown in Examples 1 to 4. Table 15 shows the electromagnetic transfer characteristics of respective media evaluated by the head in which  $T_{wr} = 0.33 \mu\text{m}$ . As for each of the media other than the medium of the sample No. 508 in which the thickness of the lower magnetic layer was 6 nm, the  $N_d/S_o$  was as low as 0.04  $\mu\text{V}_{rms}/\mu\text{V}_{pp}$  or less, and the media  $S/N$  was as large as 22.0 dB or more. From the fact that the highest  $S/N$  is obtainable when the thickness of the lower magnetic layer is 1 nm, it has been shown that the optimum value of the thickness of the lower magnetic layer also depends upon the composition of the upper magnetic layer.

[0055]

Table 13

| Sample No. | Substrate temperature (°C) | Second underlayer Cr-20at% Ti (nm) | Lower magnetic layer Co-24at% Ru-8at% B (nm) | Intermediate layer Ru (nm) | Upper magnetic layer Co-20at% Cr-14at% Pt-6at% B (nm) |
|------------|----------------------------|------------------------------------|--|----------------------------|---|
| 501        | 270                        | 20                                 | 2.0  | 0.4                        | 18.0  |
| 502        | 300                        | ↑                                  | ↑  | ↑                          | ↑   |
| 503        | 330                        | 25                                 | ↑  | ↑                          | ↑   |
| 504        | ↑                          | 15                                 | ↑  | ↑                          | ↑   |
| 505        | ↑                          | ↑                                  | ↑  | 0.6                        | ↑   |
| 506        | ↑                          | ↑                                  | ↑  | 0.4                        | ↑   |
| 507        | ↑                          | ↑                                  | ↑  | 0.2                        | ↑   |
| 508        | ↑                          | ↑                                  | 6.0  | ↑                          | ↑   |
| 509        | ↑                          | ↑                                  | 4.0  | ↑                          | ↑   |
| 510        | ↑                          | ↑                                  | 1.0  | ↑                          | ↑   |
| 511        | ↑                          | ↑                                  | 2.0  | ↑                          | 16.5  |
| 512        | ↑                          | ↑                                  | ↑  | ↑                          | 19.5  |

Table 14

| Sample No. | Hc (kA/m) | S*   | Br·t (T·nm) | Ku·v/kT |
|------------|-----------|------|-------------|---------|
| 501        | 284       | 0.61 | 5.2         | 96      |
| 502        | 306       | 0.59 | 5.1         | 110     |
| 503        | 329       | 0.61 | 5.0         | 128     |
| 504        | 279       | 0.45 | 4.8         | 98      |
| 505        | 302       | 0.48 | 4.9         | 119     |
| 506        | 305       | 0.54 | 4.8         | 120     |
| 507        | 303       | 0.45 | 4.8         | 122     |
| 508        | 202       | 0.23 | 2.7         | 95      |
| 509        | 251       | 0.46 | 3.6         | 108     |
| 510        | 313       | 0.46 | 5.2         | 115     |
| 511        | 295       | 0.41 | 4.6         | 116     |
| 512        | 305       | 0.48 | 5.4         | 122     |

Table 15

| Sample No. | So<br>( $\mu\text{Vpp}$ ) | PW50<br>(nm) | OW<br>(dB) | ReMF<br>(%) | Nd/So<br>( $\mu\text{Vrms}/\mu\text{Vpp}$ ) | Media<br>S/N (dB) |
|------------|---------------------------|--------------|------------|-------------|---|-------------------|
| 501        | 1184                      | 128          | 37         | 48          | 0.0377                                      | 22.1              |
| 502        | 1140                      | 127          | 37         | 48          | 0.0367                                      | 22.3              |
| 503        | 1105                      | 128          | 38         | 48          | 0.0381                                      | 22.0              |
| 504        | 1071                      | 128          | 39         | 47          | 0.0358                                      | 22.4              |
| 505        | 1113                      | 128          | 38         | 48          | 0.0369                                      | 22.3              |
| 506        | 1103                      | 127          | 38         | 48          | 0.0366                                      | 22.3              |
| 507        | 1108                      | 129          | 38         | 47          | 0.0371                                      | 22.1              |
| 508        | 646                       | 111          | 39         | 56          | 0.0595                                      | 19.5              |
| 509        | 844                       | 121          | 42         | 48          | 0.0360                                      | 22.5              |
| 510        | 1170                      | 128          | 38         | 47          | 0.0368                                      | 22.2              |
| 511        | 1043                      | 125          | 39         | 49          | 0.0365                                      | 22.5              |
| 512        | 1188                      | 131          | 37         | 47          | 0.0374                                      | 22.0              |

## &lt;Example 6&gt;

The media each having the same layer

5 configuration in Example 5 were manufactured, except  
that a Co-18at% Cr-14at% Pt-6at% B-2at% Cu alloy was  
used for the upper magnetic layer. Table 16 shows the  
set values of (1) the substrate temperature, (2) the  
thickness of the second underlayer, (3) the thickness  
10 of the lower magnetic layer, (4) the thickness of the  
Ru intermediate layer, and (5) the thickness of the  
upper magnetic layer. The Co-Cr-Pt-B-Cu alloy used for  
the upper magnetic layer in this example has a  
saturation magnetic flux density which is about 20 %  
15 higher than that of the Co-Cr-Pt-B alloy used in  
Example 5. Therefore, the standard thickness of the  
upper magnetic layer was set at 15.0 nm. The magnetic  
characteristics of the respective media shown in Table  
16 are shown in Table 17. It was possible to obtain

media each having a high coercivity of 240 kA/m or more except for the sample No. 608. Further, from the comparison between the medium of a sample No. 612 and the medium of a sample No. 511 of Example 5, it has been shown that, when an equal thickness is adopted, use of the Co-Cr-Pt-B-Cu alloy of this example for the upper magnetic layer provides a higher coercivity and a higher  $K_u \cdot v/kT$  than with the use of the Co-Cr-Pt-B alloy of Example 5.

[0056]

Table 16

| Sample No. | Substrate temperature (°C) | Second underlayer Cr-20at% Ti (nm) | Lower magnetic layer Co-24at% Ru-8at% B (nm) | Intermediate layer Ru (nm) | Upper magnetic layer Co-18at% Cr-14at% Pt-6at% B-2at% Cu (nm) |
|------------|----------------------------|------------------------------------|--|----------------------------|---|
| 601        | 270                        | 20                                 | 2.0  | 0.4                        | 15.0  |
| 602        | 300                        | ↑                                  | ↑  | ↑                          | ↑   |
| 603        | 330                        | 25                                 | ↑  | ↑                          | ↑   |
| 604        | ↑                          | 15                                 | ↑  | ↑                          | ↑   |
| 605        | ↑                          | ↑                                  | ↑  | 0.6                        | ↑   |
| 606        | ↑                          | ↑                                  | ↑  | 0.4                        | ↑   |
| 607        | ↑                          | ↑                                  | ↑  | 0.2                        | ↑   |
| 608        | ↑                          | ↑                                  | 6.0  | ↑                          | ↑   |
| 609        | ↑                          | ↑                                  | 4.0  | ↑                          | ↑   |
| 610        | ↑                          | ↑                                  | 1.0  | ↑                          | ↑   |
| 611        | ↑                          | ↑                                  | 2.0  | ↑                          | 13.5  |
| 612        | ↑                          | ↑                                  | ↑  | ↑                          | 16.5  |

Table 17

| Sample No. | Hc<br>(kA/m) | S*   | Br·t<br>(T·nm) | Ku·v/Kt |
|------------|--------------|------|----------------|---------|
| 601        | 270          | 0.63 | 4.8            | 97      |
| 602        | 287          | 0.54 | 4.5            | 104     |
| 603        | 322          | 0.42 | 4.6            | 121     |
| 604        | 247          | 0.49 | 4.4            | 97      |
| 605        | 287          | 0.41 | 4.7            | 114     |
| 606        | 291          | 0.39 | 4.6            | 113     |
| 607        | 293          | 0.38 | 4.8            | 115     |
| 608        | 183          | 0.14 | 2.1            | 95      |
| 609        | 246          | 0.39 | 3.4            | 108     |
| 610        | 303          | 0.43 | 5.0            | 116     |
| 611        | 277          | 0.38 | 4.2            | 105     |
| 612        | 308          | 0.48 | 4.9            | 125     |

Table 18 shows the electromagnetic transfer characteristics of each disk. The head used for the evaluation has a write gap length 0.14  $\mu\text{m}$ , a shield gap length of 0.10  $\mu\text{m}$ , and a  $T_{wr} = 0.33 \mu\text{m}$ . The head flying height  $h_m$  (the distance between the surface of the upper magnetic layer and the surface of the main pole) was set at 24 nm, and the circumferential speed was set at 7 m/s. The medium (sample No. 604) in which the thickness of the second underlayer had been decreased to 10 nm, and the medium (sample No. 609) in which the thickness of the lower magnetic layer had been decreased to 4.0 nm showed the lowest Nd/So, and a high media S/N of 22.6 dB or more. Table 19 shows the results when the measurements have been carried out by using another head in which the write gap length and the shield gap length have been the same as before, and the  $h_m$  has been set at 23 nm. Also in this case,

relatively lower Nd/So values were obtained for the media of the sample Nos. 604 and 609.

[0057]

Table 18

| Sample No. | So<br>( $\mu$ Vpp) | PW50<br>(nm) | OW<br>(dB) | ReMF<br>(%) | Nd/So<br>( $\mu$ Vrms/ $\mu$ Vpp) | Media<br>S/N (dB) |
|------------|--------------------|--------------|------------|-------------|-----------------------------------|-------------------|
| 601        | 1711               | 129          | 39         | 50          | 0.0395                            | 22.1              |
| 602        | 1660               | 129          | 39         | 49          | 0.0379                            | 22.3              |
| 603        | 1611               | 129          | 38         | 50          | 0.0382                            | 22.2              |
| 604        | 1576               | 130          | 40         | 48          | 0.0353                            | 22.6              |
| 605        | 1609               | 130          | 39         | 48          | 0.0368                            | 22.3              |
| 606        | 1581               | 130          | 40         | 49          | 0.0369                            | 22.4              |
| 607        | 1621               | 130          | 40         | 48          | 0.0367                            | 22.3              |
| 608        | 807                | 114          | 41         | 56          | 0.0699                            | 18.1              |
| 609        | 1180               | 124          | 41         | 49          | 0.0352                            | 22.8              |
| 610        | 1664               | 129          | 40         | 49          | 0.0373                            | 22.4              |
| 611        | 1415               | 127          | 41         | 50          | 0.0371                            | 22.5              |
| 612        | 1677               | 132          | 38         | 47          | 0.0374                            | 22.0              |

5

Table 19

| Sample No. | So<br>( $\mu$ Vpp) | PW50<br>(nm) | OW<br>(dB) | ReMF<br>(%) | Nd/So<br>( $\mu$ Vrms/ $\mu$ Vpp) | Media<br>S/N (dB) |
|------------|--------------------|--------------|------------|-------------|-----------------------------------|-------------------|
| 604        | 1113               | 127          | 39         | 50          | 0.0379                            | 22.4              |
| 606        | 1142               | 126          | 39         | 51          | 0.0388                            | 22.4              |
| 608        | 610                | 99           | 40         | 58          | 0.0734                            | 18.0              |
| 609        | 850                | 120          | 42         | 51          | 0.0374                            | 22.7              |
| 610        | 1212               | 126          | 39         | 50          | 0.0388                            | 22.3              |
| 611        | 1046               | 124          | 40         | 51          | 0.0385                            | 22.4              |
| 612        | 1236               | 129          | 38         | 50          | 0.0395                            | 22.0              |

#### <Example 7>

The media each having the same layer configuration in Example 1 were manufactured, except that a Ni-20at% Cr-10at% Zr alloy was used for the first underlayer, and a Cr-40 at% MoB alloy was used for the second underlayer, and a 2 to 6 nm-thick Co-16at% Ru, Co-16at% Ru-3at% B, Co-16at% Ru-10at% B, Co-

10

16at% Ru-20at% B, Co-16at% Ru-23at% B, Co-30at% Ru-8at%  
B, Co-3at% Ru-8at% B, Co-10at% Ru-5at% Cr, Co-3at% Ru-  
18at% Cr-6at% B, Co-14at% Ru-5at% C, or Co-14at% Ru-  
5at% Cr-5at% C alloy was used for the lower magnetic  
5 layer. A 19 nm-thick Co-16at% Cr-12at% Pt-12at% B  
alloy was used for the upper magnetic layer. Whereas,  
as a comparative example, a medium in which a Ru-free  
Co-18at% Cr-9at% Pt-6at% B alloy was used for the lower  
magnetic layer was manufactured. Each magnetization  
10 curve was measured, and, for any of the media, steps  
have been observed in the area in which the magnetic  
field is positive in the magnetization curve. This has  
indicated that the magnetizations of the upper magnetic  
layer and the lower magnetic layer are oriented in  
15 antiparallel to each other in the residual  
magnetization state. Table 20 shows the  
electromagnetic transfer characteristics evaluated by  
using the magnetic head described in Example 1.



[0058]

Table 20

| Sample No.             | Lower magnetic layer       | So<br>( $\mu$ Vpp) | OW<br>(dB) | Nd/So<br>( $\mu$ Vrms/ $\mu$ Vpp) | Media<br>S/N (dB) |
|------------------------|----------------------------|--------------------|------------|-----------------------------------|-------------------|
| 701                    | Co-16at% Ru                | 1260               | 37         | 0.0371                            | 22.2              |
| 702                    | Co-16at% Ru-3at% B         | 1248               | 38         | 0.0367                            | 22.1              |
| 703                    | Co-16at% Ru-10at% B        | 1140               | 38         | 0.0339                            | 22.7              |
| 704                    | Co-16at% Ru-20at% B        | 1236               | 39         | 0.0354                            | 22.3              |
| 705                    | Co-16at% Ru-23at% B        | 1020               | 33         | 0.0595                            | 19.0              |
| 706                    | Co-30at% Ru-8at% B         | 1284               | 35         | 0.0376                            | 22.7              |
| 707                    | Co-3at% Ru-8at% B          | 1164               | 38         | 0.0384                            | 22.5              |
| 708                    | Co-10at% Ru-5at% Cr        | 1200               | 40         | 0.0389                            | 22.4              |
| 709                    | Co-3at% Ru-18at% Cr-6at% B | 1188               | 41         | 0.0391                            | 21.6              |
| 710                    | Co-14at% Ru-5at% C         | 1248               | 37         | 0.0397                            | 22.5              |
| 711                    | Co-14at% Ru-5at% Cr-5at% C | 1260               | 39         | 0.0405                            | 22.5              |
| Comparative<br>example | Co-18at% Cr-9at% Pt-6at% B | 1212               | 33         | 0.0448                            | 20.2              |

For the media of the sample Nos. 701 and 702  
5 shown in Table 20, the crystal grain sizes of each  
upper magnetic layer were observed by means of a  
transmission electron microscope with an acceleration  
voltage of 200 kV. Then, the mean grain size was  
estimated in the following manner. First, the area of  
10 each crystal grain was calculated by using the obtained  
lattice image magnified two million times, and the  
diameter of the perfect circle having the same area as  
this calculated area was defined as the grain size of  
the crystal grain. At this step, the area in which the  
15 lattice stripes had the same orientation was regarded  
as one crystal grain, while the crystal grains having  
such a structure (bi-crystal structure) that they were  
adjacent to each other with their c-axes intersecting  
at right angles were regarded as different crystal

grains. The grain sizes were calculated from about 150 crystal grains, and the arithmetic mean thereof was taken to be regarded as the mean grain size.

[0059]

5           The mean grain size of the upper magnetic layer was 10.3 nm for the medium of the sample No. 701. In contrast, it was 9.6 nm, i.e., about 7 % microfiner, for the medium of the sample No. 702. On the other hand, for the medium of the sample No. 705 containing B  
10   in an amount of 23 at%, it was shown from the results of the X-ray diffraction measurement that the (11.0) orientation of the magnetic layer was largely deteriorated. It has been shown from the foregoing description as follows. Namely, in order to largely  
15   reduce the media noise by making fine the magnetic grain size, the B content of the lower magnetic layer is more desirably set at not less than 3 at% to not more than 20 at%.

[0060]

20           Whereas, for both the medium (sample No. 706) having a Ru content of 30 at% and the medium (sample No. 707) having a Ru content of 3 at%, the noise was low. This has indicated that it is possible to obtain a low noise medium if the Ru content of the lower magnetic  
25   layer falls within a range of 3 at% to 30 at%.

[0061]

As for the media (sample Nos. 708 and 709) in each of which the lower magnetic layer contained Cr,

the overwrite characteristic was particularly good. Whereas, for the media (sample Nos. 710 and 711) in each of which C in place of B was added to the lower magnetic layer, the media noise was slightly higher, but the output resolution was high, and a high S/N was shown. On the other hand, for the medium in which a Co-20 at% Cr-12at% Pt-6 at% B alloy was used for the lower magnetic layer of the comparative example, the overwrite characteristic was bad, and the media noise was also high.

[0062]

<Example 8>

A 35 nm-thick Ni-30at% Nb alloy layer was formed as each first underlayer, and a 10 nm-thick Cr-15at% Ti alloy layer was formed as each second underlayer. Then, as each third underlayer, a 3 nm-thick Co-34at% Cr alloy layer was formed. Subsequently, as each lower magnetic layer, the layer of Co-4at% Re, Co-8at% Re-11at% B, Co-6at% Re-5at% Cr, Co-5at% Re-5at% Cr-6at% B, Co-12at% Re-8at% C, or Co-4at% Re-4at% B-4at% C alloy layer was formed with a thickness of 2 to 6 nm. Thereafter, a 18 nm-thick Co-20at% Cr-11at% Pt-7at% B alloy layer was formed via a 0.4 nm-thick Ru intermediate layer.

[0063]

Each magnetization curve was measured by applying a magnetic field in the in-plane direction, and steps have been observed in the area in which the magnetic

field is positive. This has indicated that the magnetizations of the upper magnetic layer and the lower magnetic layer are oriented in antiparallel to each other in the residual magnetization state. Table 21 shows the electromagnetic transfer characteristics evaluated by using the same magnetic head as that described in Example 1. Any of the media exhibited a high media S/N of 21 dB or more.

[0064]

Table 21

| Sample No. | Lower magnetic layer      | So<br>( $\mu$ Vpp) | OW<br>(dB) | Nd/So<br>( $\mu$ Vrms/ $\mu$ Vpp) | Media S/N<br>(dB) |
|------------|---------------------------|--------------------|------------|-----------------------------------|-------------------|
| 801        | Co-4at% Re                | 1358               | 34         | 0.0385                            | 21.2              |
| 802        | Co-8at% Re-11at% B        | 1302               | 35         | 0.0347                            | 21.9              |
| 803        | Co-6at% Re-5at% Cr        | 1456               | 37         | 0.0377                            | 21.3              |
| 804        | Co-5at% Re-5at% Cr-6at% B | 1470               | 38         | 0.0402                            | 21.0              |
| 805        | Co-12at% Re-8at% C        | 1414               | 33         | 0.0413                            | 21.1              |
| 806        | Co-6at% Re-6at% Cr-8at% C | 1442               | 33         | 0.0399                            | 21.2              |
| 807        | Co-4at% Re-4at% B-4at% C  | 1456               | 33         | 0.0403                            | 21.3              |

#### <Example 9>

As each first underlayer, a 100 nm-thick Ni-50 at% Al alloy layer was formed, and as each second underlayer, a 25 nm-thick Cr-50 at% V alloy layer was formed. Then, the third underlayer was not provided, and each magnetic layer and each protective layer were successively deposited directly thereon. The first underlayer was formed on a 50 nm-by-50 nm basis in two separate chambers in such a manner as to be formed with a thickness of 50 nm each in respective ones of the two chambers. The substrate heating was carried out prior

to formation of the underlayer so that the substrate temperature was 280 °C. The deposition conditions for respective layers were the same as in Example 1, and the layer configuration of the magnetic layer and the Ru intermediate layer was the same as that of the medium of the sample No. 114. The X-ray diffraction measurement was carried out, and only the diffraction peak from the (10.0) plane was observed from the magnetic layer. This has indicated that it is the (10.0)-oriented medium. Further, in the magnetization curve, steps have been observed in the area in which the magnetic field is positive. This has indicated that the magnetizations of the upper magnetic layer and the lower magnetic layer are oriented in antiparallel to each other in the residual magnetization state. The coercivity, the  $S^*$ , and the  $Br \cdot t$  were 303 kA/m, 0.70, and 4.8 T·nm, respectively, and the  $K_u \cdot v/kT$  was 105. The electromagnetic transfer characteristics were evaluated by using the same magnetic head as in Example 1. As a result, the normalized media noise was 0.0365  $\mu V_{rms}/\mu V_{pp}$ , and the media S/N was 22.0 dB. Thus, such good results were obtained.

[0065]

<Example 10>

A NiP-plated Al-Mg alloy substrate was heated up to 220 °C. Then, as the underlayers, a 10 nm-thick Cr layer, a 20 nm-thick layer of alloy of Cr containing B in an amount of 0 to 12 at%, and a 5 nm-thick Co-37at%

Cr alloy layer were successively stacked. Subsequently, the magnetic layer and the protective layer were successively formed. As the B-containing Cr alloy, Cr-40at% Mo-2at% B, Cr-40at% Mo-4at% B, Cr-40at% Mo-6at% B, Cr-40at% Mo-8at% B, Cr-40at% Mo-10at% B, or Cr-40at% Mo-12at% B was used. As a comparative example, a medium using a Cr-40at% Mo alloy not containing B was manufactured. The layer configuration of the magnetic layer and the Ru intermediate layer was the same as that of the medium of the sample No. 214. In each of the media of this example, the Al-Mg alloy substrate is used. Therefore, the first underlayer for causing the Cr alloy to be (100)-oriented is not formed. Further, in order to ensure the compatibility between the intensive (100) orientation and the microfine crystal grains, the second underlayer made of the Cr alloy was so configured as to have a double layered structure. [0066]

The X-ray diffraction measurement of each of the media of this example was carried out. As a result, for all the media other than the medium using the Cr-40at% Mo-12at% B underlayer, there were observed the diffraction peaks from the (100) planes of Cr and the CrMoB alloy underlayers, and intensive diffraction peaks from the (11.0) planes of the third underlayers and the magnetic layers. For the medium using the Cr-40at% Mo-12at% B underlayer, the diffraction peak from the (11.0) plane of the magnetic layer was very weak,

and an intensive (00.2) peak was observed. This has indicated that, for the medium using the Cr-40at% Mo-12at% B underlayer, the in-plane component of the c-axis is reduced.

5 [0067]

FIGS. 5(a) and 5(b) show the relationships of the B concentration of the CrMoB underlayer with the coercivity  $H_c$ , and the normalized media noise  $N_d/S_o$ , respectively. Herein, the normalized media noise is  
10 the value evaluated by using the same magnetic head as in Example 1. The coercivity  $H_c$  decreases with an increase in B content, and sharply decreases over a range of 10 at% to 12 at%. On the other hand, the normalized media noise  $N_d/S_o$  once decreases with an  
15 increase in B content, becomes minimum with respect to the B content of 6 at% to 8 at%, and then sharply increases. This has indicated as follows. Namely, in order to obtain a medium having a high coercivity of 240 kA/m or more and a low media noise of 0.04  
20  $\mu V_{rms}/\mu V_{pp}$  or less, it is desirable that the B content of the CrMoB alloy underlayer is set at 2 at% to 10 at%.  
[0068]

<Example 11>

Out of the magnetic recording media 91 described  
25 in Examples 1 to 10, the media of the sample Nos. 113, 208, 213, 304, 404, 511, 609, 703, and 802, the medium shown in Example 9, and the medium using the Cr-40at% Mo-8at% B underlayer in Example 10 were selected. Then,

a magnetic storage apparatus was configured as shown in FIG. 6, which had each of these media, a driver 92 for driving the magnetic recording medium, a magnetic head 93 made up of a write element and a read element, means 94 for causing the magnetic head to perform relative movement with respect to the magnetic recording medium, and a read / write signal processing means 95 for performing the signal input to the magnetic head and output signal read-back from the magnetic head, and a station unit 96 for shelter during unloading.

[0069]

The read element of the magnetic head was made up of a magnetoresistive head. FIG. 7 is a schematic perspective view showing the configuration of the magnetic head. This head is a composite head having both the inductive head for writing and the magnetoresistive head for reading formed on a substrate 801. The writing head is made up of an upper magnetic pole 803 and a lower magnetic pole-cum-upper shield layer 804 with a coil 802 interposed therebetween. The gap length between the two magnetic poles was set at 0.14  $\mu\text{m}$ . Further, a 1.5  $\mu\text{m}$ -thick copper wire was used for the coil. The reading head was made up of a magnetoresistive sensor 805 and electrode patterns 806 on opposite sides thereof. The magnetoresistive sensor was interposed between the lower magnetic pole-cum-upper shield layer 804 and a lower shield layer 807.



The distance between the two shield layers was set at 0.10  $\mu\text{m}$ . Incidentally, in this figure, the gap layer between the magnetic poles and the gap layer between the shield layer and the magnetoresistive sensor are omitted.

[0070]

FIG. 8 shows the cross sectional configuration of the magnetoresistive sensor. A signal sensing region 900 of the magnetic sensor is configured with a magnetoresistive sensor (spin-valve type read element) including a plurality of conductive magnetic layers of which mutual magnetization directions relatively change due to the external magnetic field, thereby generating a large resistance change, and conductive non-magnetic layers disposed each between the conductive magnetic layers. This magnetic sensor is so configured that on a gap layer 901, a Ta buffer layer 902, a lower magnetic layer 903, an intermediate layer 904 configured with copper, an upper magnetic layer 905, and an anti-ferromagnetic layer 906 made of a Pt-Mn alloy are successively formed. A Ni-20at% Fe alloy was used for the lower magnetic layer, and cobalt was used for the upper magnetic layer. The magnetization of the upper magnetic layer is fixed in one direction due to the exchange field from the anti-ferromagnetic layer. In contrast, the direction of the magnetization of the lower magnetic layer in contact with the upper magnetic layer via the non-magnetic layer is changed due to the

leakage field from the magnetic recording medium, so that the resistance change occurs. There are tapered regions 907 each processed in tapered form on opposite sides of the signal sensing region. The tapered regions are made up of permanent magnet layers 908 for converting the lower magnetic layer into a single domain, and a pair of electrodes 806 for taking a signal formed thereon. The permanent magnet layer is required to have a large coercivity and have a magnetization direction not changing with ease. For this reason, a Co-Cr-Pt alloy was used.

[0071]

Out of the magnetic recording media 91 described in Examples 1 to 8, the media of the sample Nos. 113, 208, 213, 304, 404, 511, 609, 703, and 802, the medium shown in Example 9, and the medium using the Cr-40at% Mo-8at% B underlayer in Example 10 were selected. Then, each medium was used in combination with the head shown in FIG. 7 to configure the magnetic storage apparatus shown in FIG. 6. By the magnetic storage apparatus configured in this manner even if any of the media was used, it was possible to achieve a recording density of 50 Mbit/mm<sup>2</sup> or more.

[0072]

In this example, there was used a magnetic head in which the magnetoresistive head was formed on the magnetic head slider having an air bearing surface rail area of 1.4 mm<sup>2</sup> or less and a mass of 2 mg or less. By

setting the area of the air bearing surface rail of the slider at  $1.4 \text{ mm}^2$  or less, and further setting the mass at 2 mg or less, it was possible to improve the shock resistance reliability. In consequence, it was possible to ensure the compatibility between the high recording density and the high shock resistance. Accordingly, it was possible to implement a mean time between failures (MTBF) of 300,000 hours or more with a recording density of 50 Mbit/ $\text{mm}^2$  or more.

[0073]

[Effects of the Invention]

The magnetic recording medium of the present invention has effects of reducing the media noise and improving the stability against the thermal fluctuation. By using the magnetic recording medium of the present invention and the magnetoresistive head, it becomes possible to implement a magnetic storage apparatus having an areal recording density of 50 Mbit/ $\text{mm}^2$  or more, and a mean time between failures of 300,000 hours or more.

[Brief Description of the Drawings]

[FIG. 1]

This is a graph showing a hysteresis loop of a medium of one example of the present invention;

[FIG. 2]

This is a schematic diagram showing one example of a cross sectional structure of a magnetic recording medium of the present invention;

[FIG. 3]

This is a schematic diagram showing the configuration of a disc formation apparatus used in the present invention;

5 [FIG. 4]

This is an enlarged view of a portion at a magnetic field of around zero of the hysteresis loop of a medium of one example of the present invention;

[FIG. 5]

10 (a) and (b) are graphs respectively showing the relationships of the coercivity, and the normalized media noise with the B content of the underlayer of a medium of one example of the present invention;

[FIG. 6]

15 This is a perspective view showing one example of a magnetic storage apparatus of the present invention;

[FIG. 7]

This is a perspective view showing one example of the cross sectional structure of a magnetic head in the magnetic storage apparatus of the present invention;  
20 and

[FIG. 8]

This is a schematic diagram showing one example of the cross sectional structure of a magnetoresistive sensor unit of the magnetic head in the magnetic  
25 storage apparatus of the present invention.

[Description of the Reference Numerals]

11: substrate

12: first underlayer

|    |   |                                 |
|----|---|---------------------------------|
|    | 13: second underlayer   | 14: third underlayer            |
|    | 15: lower magnetic layer  | 16: intermediate layer          |
|    | 17: upper magnetic layer  | 18: protective layer            |
|    | 19: lubricant layer   | 20: charging chamber            |
| 5  | 21: first underlayer forming chamber                                    |                                 |
|    | 22: heating chamber   |                                 |
|    | 23: second underlayer forming chamber                                   |                                 |
|    | 24: third underlayer forming chamber                                    |                                 |
|    | 25: lower magnetic layer forming chamber                                |                                 |
| 10 | 26: intermediate layer forming chamber                                  |                                 |
|    | 27: upper magnetic layer forming chamber                                |                                 |
|    | 28: protective layer forming chamber                                    |                                 |
|    | 28': protective layer forming chamber                                   |                                 |
|    | 29: discharging chamber   | 30: main chamber                |
| 15 | 91: magnetic recording media  |                                 |
|    | 92: driver for driving a magnetic recording medium                      |                                 |
|    | 93: magnetic head   | 94: magnetic head driving means |
|    | 95: signal processing means for recording or reproducing signal         |                                 |
| 20 | 96: station unit for shelter during unloading                           |                                 |
|    | 802: coil   | 803: upper magnetic pole        |
|    | 804: lower magnetic pole-cum-upper shield layer                         |                                 |
|    | 805: magnetoresistive sensor  |                                 |
|    | 806: electrode pattern  | 807: lower shield layer         |
| 25 | 900: signal sensing region  |                                 |
|    | 901: gap layer between the shield layer and the magnetoresistive sensor |                                 |
|    | 902: buffer layer   |                                 |
|    | 903: lower magnetic layer   | 904: intermediate layer         |

905: lower magnetic layer

906: anti-ferromagnetic layer      907: tapered region

908: permanent magnet layer

[Type of the Document] Abstract of the Disclosure

[Abstract]

[Purpose] It is an object of the present invention to provide a high reliability magnetic storage apparatus  
5 capable of performing writing and reading back of highly dense information.

[Solving Means]

The magnetic storage apparatus is so configured as to have a longitudinal magnetic recording medium  
10 including: a magnetic layer formed on a non-magnetic substrate via a plurality of underlayers; the magnetic layer including a lower magnetic layer containing Ru or Re in an amount of not less than 3 at% to not more than 30 at%, and Cr in an amount of not less than 0 at% to  
15 not more than 18 at%, and further containing at least one of B or C in an amount of not less than 0 at% to not more than 20 at%, and an upper magnetic layer containing Co as a main component disposed thereon via a non-magnetic intermediate layer; a driver for driving  
20 it in the recording direction; a composite magnetic head in which the read element is configured with a spin-valve type sensor; means for causing the magnetic head to perform relative movement with respect to the magnetic recording medium; and a read / write signal  
25 processing means for performing the signal input to the magnetic head and output signal read-back from the magnetic head.

[Selected Figure] FIG. 2



1/4

**FIG. 1**

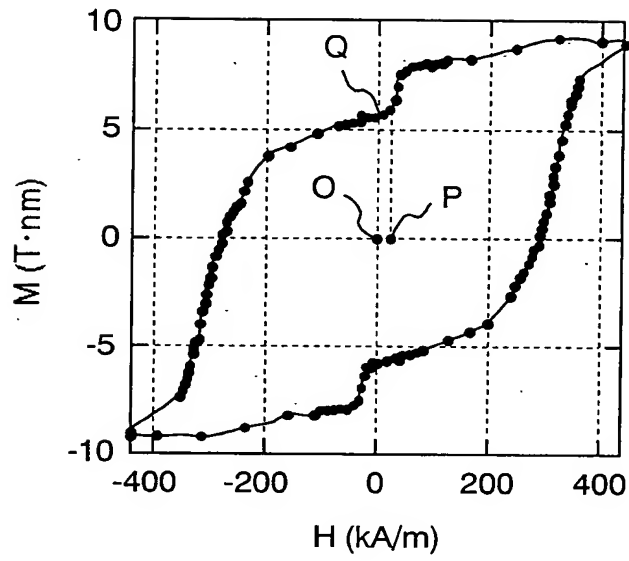


**FIG. 2**

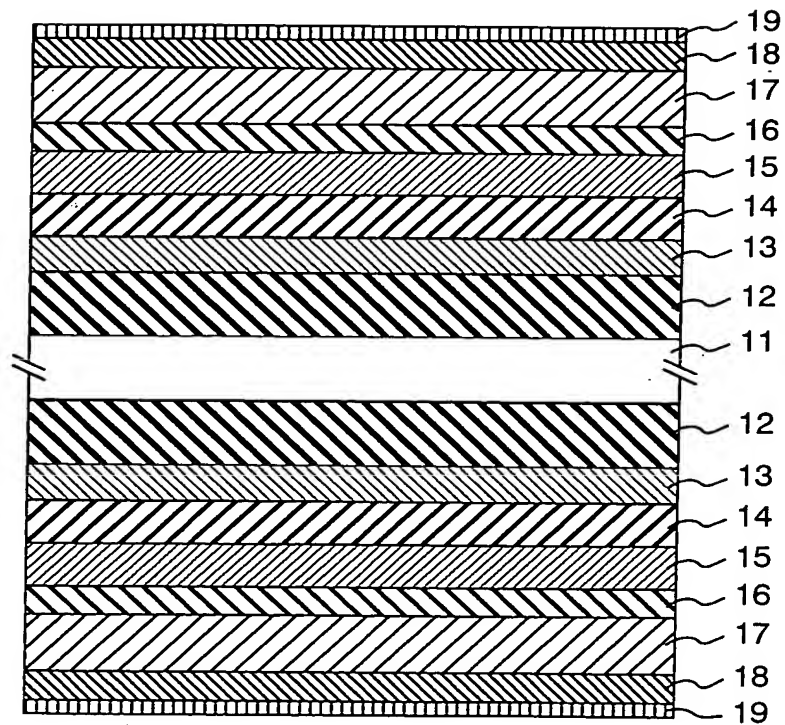




**FIG. 3**

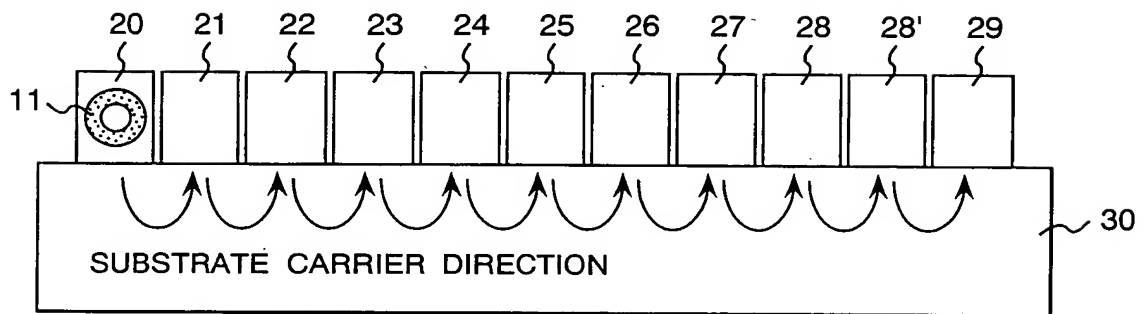
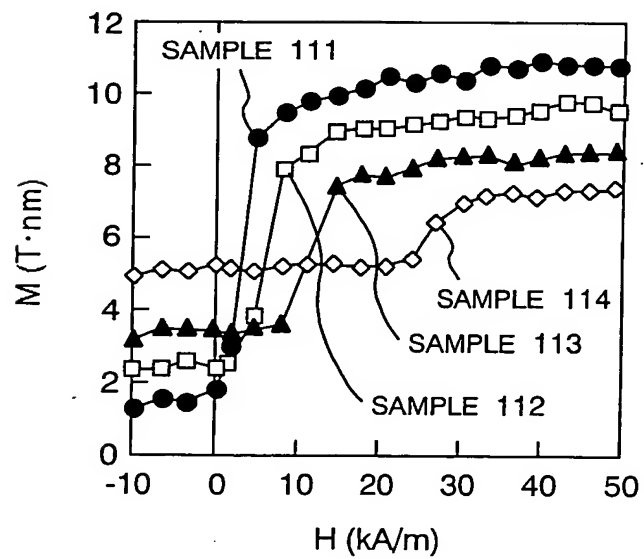


**FIG. 4**





3/4

**FIG. 5a**

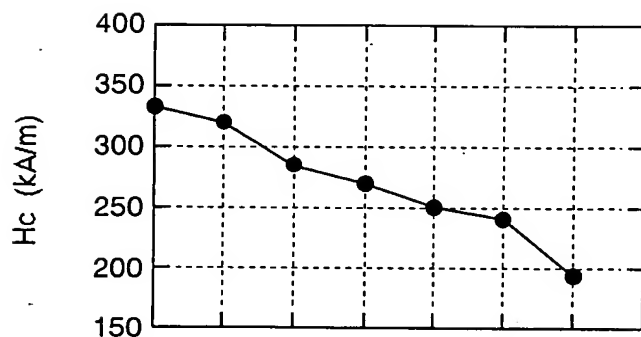


**FIG. 5b**

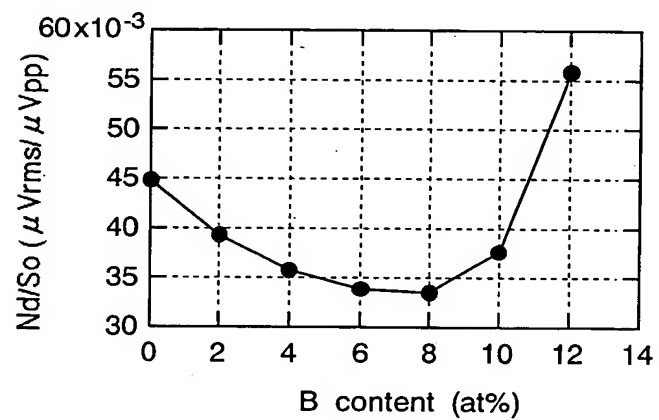


**FIG. 6**

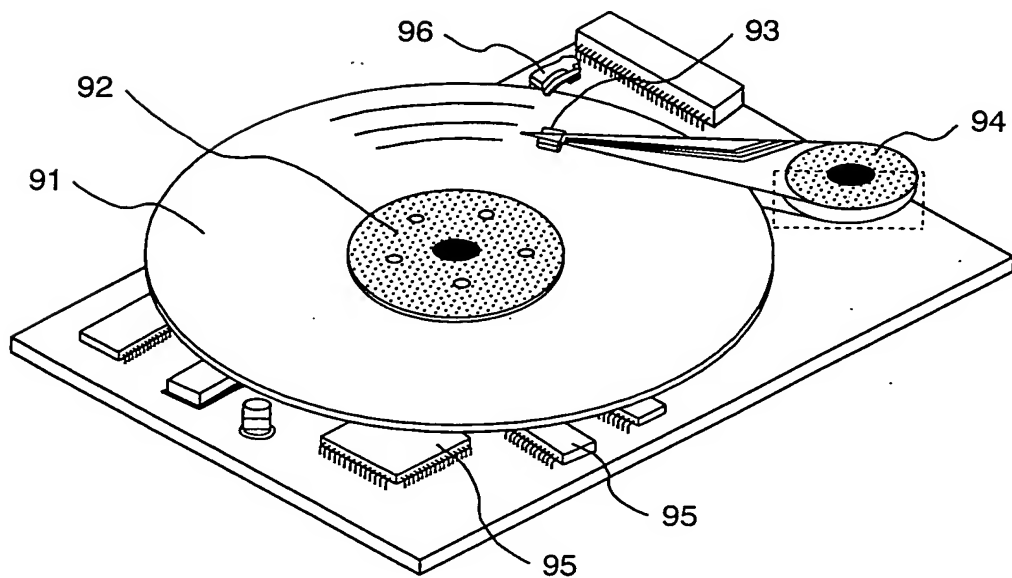




**FIG. 7**

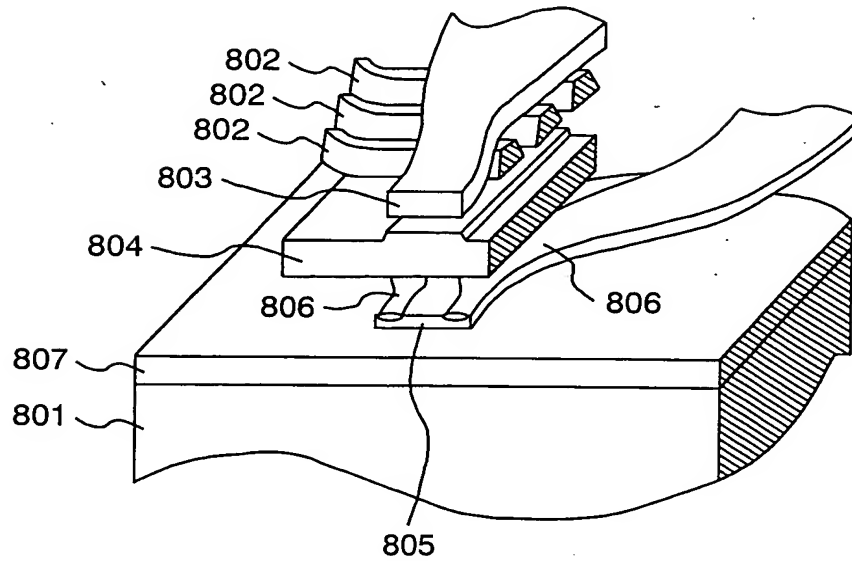


**FIG. 8**

